A POLARIMETRIC RADAR VIEW AT EXPOSED INTERTIDAL FLATS

Martin Gade

Universität Hamburg, Institut für Meereskunde, Hamburg, Germany

ABSTRACT

We analyzed a large amount of high-resolution Synthetic Aperture Radar (SAR) data of exposed intertidal flats on the German North Sea coast with respect to the imaging of sediments, macrophytes, and mussels. TerraSAR-X and Radarsat-2 images of four test areas acquired from 2008 to 2013 form the basis for the present investigation and are used to demonstrate that pairs of SAR images, if combined through basic algebraic operations, can already provide indicators for bivalve (oyster and mussel) beds. Our results show evidence that single-acquisition, dual-polarization SAR imagery can be used in this respect. The polarization coefficient (i.e., the normalized difference polarization ratio) can be used to infer indicators for oyster and blue-mussel beds.

***Index Terms*—** intertidal flats, bivalve beds, SAR, radar polarization, coastal habitats

1. INTRODUCTION

Intertidal flats are coastal areas that fall dry once during each tidal cycle. Large intertidal flats can be found in Europe, e.g. on the Dutch, German, and Danish North Sea coasts, on the U.K. east and west coasts, and along the French Atlantic coast, and at other places worldwide, e.g. in South Korea and northwest Africa. Adopting the Dutch name those areas are often referred to as Wadden Seas. Since 2009 the German Wadden Sea is a UNESCO World Natural Heritage, and according to national and international laws and regulations [1][2] a frequent surveillance of the entire area is mandatory.

Remote sensing techniques are ideally suited for the surveillance of areas that are difficult to access. In this respect, Synthetic Aperture Radar (SAR) sensors, because of their all-weather capabilities and their independence of daylight, may be the first choice; however, the radar imaging of bare soils is rather complex, and the very processes responsible for the backscattering of microwaves from exposed intertidal flats are still subject to ongoing research.

Within the German national project SAMOWatt (‘Satellite Monitoring of the Wadden Sea’), we analyzed SAR images of dry-fallen intertidal flats on the German North Sea coast to gain further insight into mechanisms of the radar backscattering from those flats, and to provide a basis for the inclusion of SAR data into existing classification systems, which were built solely upon optical data [3]. It was demonstrated [4] that multi-frequency SAR imagery may be used to extract surface roughness parameters of dry-fallen intertidal flats. However, the applied inversion scheme requires L-band SAR imagery, which was no longer available after the sudden end of the ALOS-1 mission in 2011. Nonetheless, it was also shown that single-frequency, multi-temporal SAR imagery can be used for the detection of bivalve (oyster) beds [5]. Here we proceed along those lines and summarize some further results obtained through the analysis of a great deal of SAR images acquired close to low tide.

2. TEST SITE AND DATA

Four test areas on the German North Sea coast were identified (Figure 1), which represent areas of typical sediment distributions on intertidal flats and which also include vegetated areas and mussel and oyster beds. Three of them, namely the test areas ‘Amrum’, ‘Pellworm’ and ‘Wesselburen’ (denoted as ‘A’, ‘P’, and ‘W’, respectively, in Figure 1) are located in the northern part of the German North Sea coast, in the German National Park ‘Schleswig-Holstein Wadden Sea’. The other test area, ‘Jadebusen’ (‘J’ in Figure 1), is located further south and is part of the German National Park ‘Lower Saxonian Wadden Sea’. Most of those test areas were already subject to previous studies [4][5], and they were complemented by the test area ‘Jadebusen’, because this bay is characterized by a high spatial variability in surface types, along with strong tidal currents.

More than 120 SAR images of the SAMOWatt test areas, acquired between July 2008 and December 2013 by SAR sensors aboard the European ENVISAT and ERS-2, the German TerraSAR-X, and the Canadian Radarsat-2 satellites, form the data basis of the analyses presented herein. Depending on the acquisition mode, the SAR

The work presented herein was partly funded by the German Ministry of Economy (BMWi) under contract 50 EE 1117 (SAMOWatt). The TerraSAR-X and Radarsat-2 data were provided by DLR and CSA, respectively, under contract 5077/OCE0994.

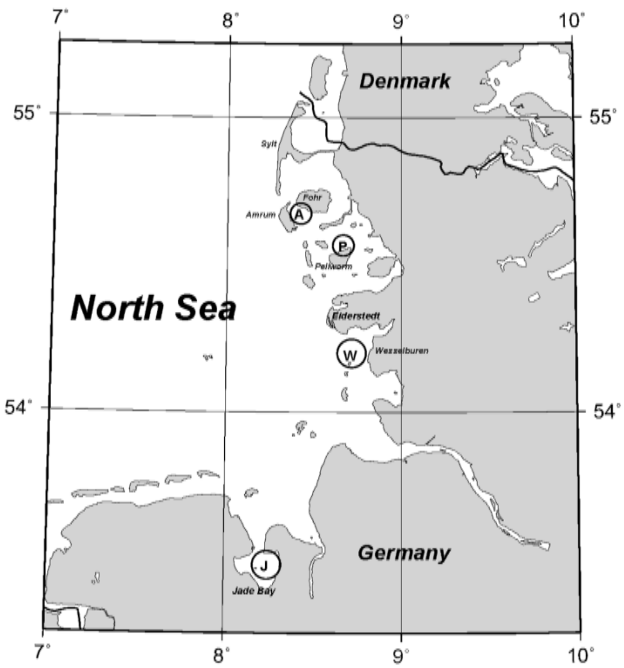

Figure 1. Four test sites on the German North Sea coast. A: 'Amrum', P: 'Pellworm', W: 'Wesselburen', and J: 'Jadebusen'.

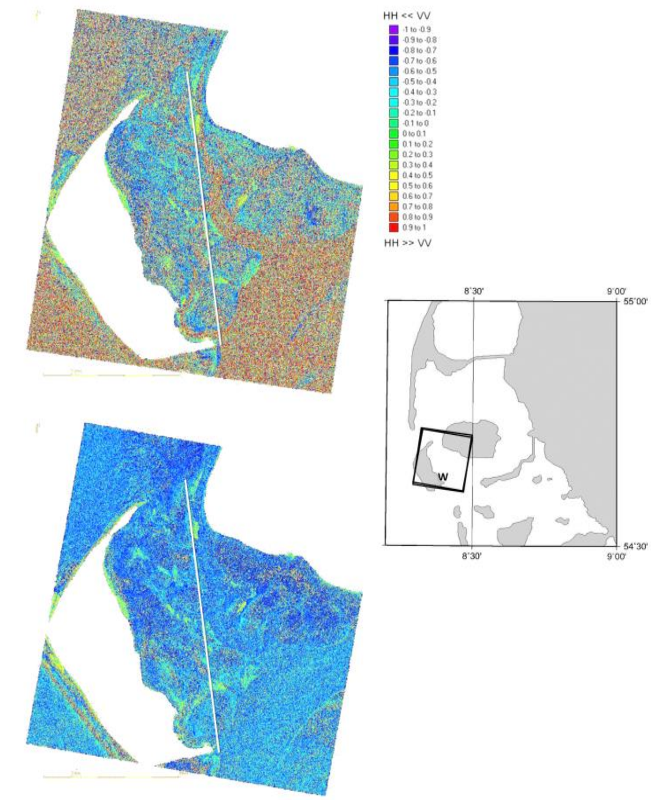

Figure 2. Polarization coefficient (normalized difference polarization ratio) calculated from dual-polarization TSX SAR images of the 'Amrum' test site acquired (upper) on June 6, 2013 and (lower) on June 22, 2013. The letter 'W' in the map on the right marks the position of the tide gauge 'Wittdün'.

systems provided imagery with pixel sizes ranging from 3 m down to 1 m, or even below, thereby allowing detailed studies of the radar backscattering from exposed intertidal flats.

3. RESULTS

We define the polarization coefficient, *PC*, as the normalized difference polarization ratio:

$$PC(SAR_{HH}, SAR_{VV}) = \frac{SAR_{HH} - SAR_{VV}}{SAR_{HH} + SAR_{VV}} \quad (1)$$

where SAR_{HH} and SAR_{VV} are the respective collocated (and calibrated) SAR image data acquired by the same sensor and at the same time, but at horizontal (HH) and vertical (VV) polarizations. Two examples are shown in Figure 3, which were both derived from pairs of HH and VV polarization TSX images of the test site 'Amrum' (11.2 km × 13.3 km), acquired on June 6, 2013, at 05:33 UTC (upper panel) and June 22, 2013, at 05:41 UTC (lower panel).

At the time of the first image acquisition (June 6, 27 minutes after low tide; upper panel) the wind conditions were 4.3 m/s / 26°, and during the second image acquisition (June 22, 35 minutes after low tide; lower panel) they were 10.0 m/s / 228°. Both islands, Amrum on the left and Föhr on the upper right, are masked out for better orientation. The open flats always appear in bluish (cyan to dark blue) colors, indicating higher backscatter at vertical polarization. Moreover, in both panels several green patches with sharp edges can be seen on the open flats, between the two islands, and coincide with oyster beds monitored during the recent field campaigns. The oysters, being arranged irregularly within the beds, with no dominant orientation, cause similar radar backscatter at both polarizations and, in turn, a polarization coefficient close to zero. We also note that this effect is independent of the imaging geometry (i.e. of the radar incidence and look angles), again, because of the oysters' heterogeneous orientation. On the other hand, the difference in radar backscatter from bare (exposed) sediments at vertical and horizontal polarizations increases with increasing incidence angle [6]. Therefore, the patches caused by oysters are more pronounced, i.e. the contrast to their vicinity is much stronger, when the images were acquired at high incidence angles (> 40°; the images used herein were acquired at mean (center) incidence angles of 51.2° and 42.6°, respectively).

Figure 3 shows transects (from north to south) along the white lines in Figure 3: the lower, blue curves correspond to a moving 11-pixel average and the upper, red curve to the corresponding (11-pixel) standard deviation. Locations of bivalve beds (recorded during the field campaigns) are marked as thick horizontal bars on the abscissa. Since the radar backscattering from bivalve beds generally does not differ much at both co-polarizations, the absolute value of the polarization coefficient (Eq. 1) is small in those areas, and so is the standard deviation. We note that bivalve beds appear to be the only areas where both the absolute mean and the standard deviation are always small, whereas exposed sediments may show mean values close to zero, but high standard deviations (see the middle part of the upper panel in Figure 3), and tidal channels may show the opposite (the dip on the right of both curves in that panel). Therefore, a more robust quantity is the product P of both,

$$P = |\mu_{PC}| \cdot \sigma_{PC} \qquad (2)$$

where μ_{PC} and σ_{PC} are the absolute value of the (running) mean and the (running) standard deviation, respectively. We added a third, green curve showing the product P. For a better visualization, all three curves were smoothed applying a boxcar filter of length 30.

In both panels of Figure 3 the mean polarization coefficient (lower, blue curve) is generally negative, indicating stronger radar backscattering at VV-polarization, which is in accordance with backscattering theories ([7] and literature cited therein). At low wind conditions, as encountered on June 6 (upper panel in Figure 2), both co-polarization channels are noisier, thereby causing a stronger variation and, therefore, a higher standard deviation of the polarization coefficient. In contrast, bivalve beds always tend to cause an increased radar backscatter at both co-polarizations [8], which results in the observed increase in the (running) mean, the decrease in the (running) standard deviation, and eventually in low absolute values of the product of both. As a result, the low values of the middle, green curves in Figure 3 coincide very well with the locations of observed bivalve beds.

Finally, we performed the same kind of analysis for all TSX SAR imagery of the 'Amrum' test site acquired in 2013: five SAR image pairs (acquired at HH- and VV-polarization) were used to calculated maps of the polarization coefficient, like those shown in Figure 2. A moving 11 pixels × 11 pixels window was applied to derive the local product P, and the resulting maps were collocated and temporally averaged. The final result, therefore, contains the same, though two-dimensional, information as the middle, green curves in Figure 3. It is shown in Figure 4 with lowest values (below 0.03) marked in dark blue.

It is obvious that the use of multi-polarization SAR imagery has some additional potential for the monitoring of intertidal flat surfaces using SAR sensors. Although the limit of 'lowest' values (0.03) was arbitrarily chosen, a comparison of Figure 4 with field observations (not shown herein) immediately reveals that the product P provides another indicator for bivalve beds on exposed intertidal flats. Moreover, and with the given color coding, areas of frequent water coverage (i.e., mainly the tidal channels, but also parts of the open flats where remnant water can often be encountered) appear in yellow and orange colors, whereas the exposed flats appear in green. More research is needed here to find out to what extent this parameter can be used in this respect.

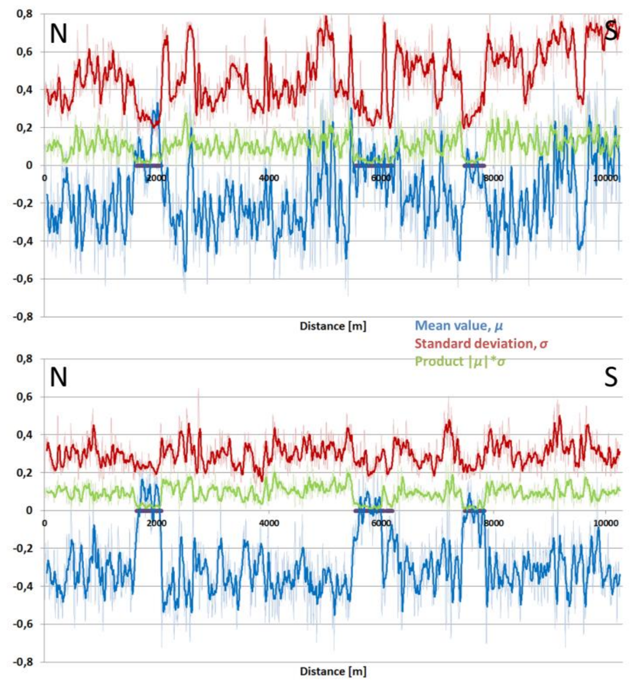

Figure 3. Profiles along the transects included in Figure 2 (from north to south); blue: mean of a moving 11-pixel window, red: respective standard deviation, green: product of the absolute mean and standard deviation.

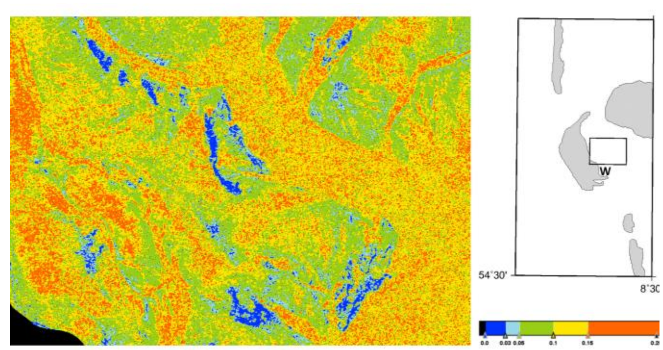

Figure 4. Product P of the absolute mean and standard deviation, each calculated for a moving window of size 11 pixels × 11 pixels. Shown is the mean value of the five TSX dual-polarization acquisitions from 2013 of a part of the 'Amrum' test site. The letter 'W' in the map marks the position of the tide gauge 'Wittdün'.

4. CONCLUSIONS

Within the national German project SAMOWatt data from multi-satellite SAR images of exposed intertidal flats have been analyzed to improve existing classification systems by including SAR data. A systematic analysis of dual-polarization SAR data from exposed intertidal flats, acquired close to low tide, provides valuable information to be used for the routine monitoring of the German Wadden Sea and may provide input for existing classification schemes.

Our results based on dual-polarization SAR images are very promising, since they allow detecting of bivalve beds, particularly when the images were acquired at incidence angles exceeding 40°, when the contrast between the backscatter from the bivalve beds and from the surrounding sediments is higher. The polarization coefficient, as introduced herein, is a parameter derived through basic algebraic operations and provides an indicator for oyster beds. Locations where the product of the polarization coefficient's spatial (absolute) mean and standard deviation is low clearly coincide with those where oyster beds were encountered during field excursions. We therefore conclude that the detection of mussel or oyster habitats seems easier when SAR data acquired at both co-polarizations are used. Moreover, the fact that this method is based on single-acquisition SAR data makes it superior to others based on series of SAR images, particularly for the monitoring of a highly dynamic environment such as intertidal flats.

Not all SAR sensors currently in orbit provide imagery at both co-polarizations simultaneously. SAR images from the recently launched Sentinel-1A may be only available at dual polarizations, i.e., a combination of one co- and one cross-polarization, along with a lower spatial resolution. A respective extension of the analyses presented herein towards the use of cross-polarization data (in which bivalve beds also show a clear signal) will be subject to future research.

5. ACKNOWLEDGMENTS

Sabrina Melchionna, Linnea Kemme, Franziska Leverenz, and Fabian Werner helped with the data processing. Tide gauge data were provided by the German Federal Waterways and Shipping Administration through the German Federal Institute of Hydrology (Bundesamt für Gewässerkunde, BfG) and by the Waterways and Shipping Board (Wasser- und Schifffahrtsamt, WSA) Tönning.

6. REFERENCES

[1] European Commission, 1992. Council Directive 92/43/EEC of 21 May 1992 on the conservation of natural habitats and of wild fauna and flora. Official J. European Communities, L 206, 22.07.1992: 1-66.

[2] European Commission, 2008. Directive 2008/56/EC of the European Parliamant and of the Council of 17 June 2008 establishing a framework for community action in the field of marine environmental policy (Marine Strategy Framework Directive). Official J. European Communities, L 164, 25.6.2008: 19-40.

[3] Brockmann, C., Stelzer, K., 2008. Optical Remote Sensing of Intertidal Flats. In: Barale V, Gade M (eds.), Remote Sensing of the European Seas. Springer, Heidelberg, 514 pp., 117-128.

[4] Gade, M., Alpers, W., Melsheimer, C., Tanck, G., 2008. Classification of sediments on exposed tidal flats in the German Bight using multi-frequency radar data. Remote Sens. Environ., 112: 1603-1613.

[5] Gade, M., Melchionna, S., Stelzer, K., Kohlus, J., 2014. Multi-Frequency SAR Data Help Improving the Monitoring of Intertidal Flats on the German North Sea Coast. Estuar. Coast. Shelf Sci., doi: 10.1016/j.ecss.2014.01.007.

[6] Fung, A.K., Chen, K.S., 2004. An update on the IEM surface backscattering model. IEEE Geoscience and Remote Sensing Letters 1, pp. 75-77.

[7] Hajnsek, I., 2001. Inversion of Surface Parameters Using Polarimetric SAR, Dissertation, Friedrich-Schiller University Jena, Institute of Geography, Department of Geoinformatik, Jena, Germany, 238 pp.

[8] Gade, M., and S. Melchionna, 2016. Joint Use of Multiple Synthetic Aperture Radar Imagery for the Detection of Bivalve Beds and Morphological Changes on Intertidal Flats. Estuar. Coast. Shelf Sci., submitted.